

## PAPER

# Highly Accurate Vegetation Loss Model with Seasonal Characteristics for High-Altitude Platform Station

Hideki OMOTE<sup>†a)</sup>, Akihiro SATO<sup>†</sup>, Sho KIMURA<sup>†</sup>, Shoma TANAKA<sup>†</sup>, and HoYu LIN<sup>†</sup>, *Members*

**SUMMARY** High-Altitude Platform Station (HAPS) provides communication services from an altitude of 20 km via a stratospheric platform such as a balloon, solar-powered airship, or other aircraft, and is attracting much attention as a new mobile communication platform for ultra-wide coverage areas and disaster-resilient networks. HAPS can provide mobile communication services directly to the existing smartphones commonly used in terrestrial mobile communication networks such as Fourth Generation Long Term Evolution (4G LTE), and in the near future, Fifth Generation New Radio (5G NR). In order to design efficient HAPS-based cell configurations, we need a radio wave propagation model that takes into consideration factors such as terrain, vegetation, urban areas, suburban areas, and building entry loss. In this paper, we propose a new vegetation loss model for Recommendation ITU-R P.833-9 that can take transmission frequency and seasonal characteristics into consideration. It is based on measurements and analyses of the vegetation loss of deciduous trees in different seasons in Japan. Also, we carried out actual stratospheric measurements in the 700 MHz band in Kenya to extend the lower frequency limit. Because the measured results show good agreement with the results predicted by the new vegetation loss model, the model is sufficiently valid in various areas including actual HAPS usage.

**key words:** mobile radio, propagation, vegetation, vegetation loss, seasonal characteristics, measurements

## 1. Introduction

High-Altitude Platform Station (HAPS) is a radio station installed on a stratospheric platform such as a balloon, solar-powered airship, or other aircraft [1], [2], that flies in the stratosphere at the altitude of approximately 20 km where low wind speeds are expected to yield stable flight as shown in Fig. 1. HAPS has the potential for mobile communications using the same systems as terrestrial networks such as 4G LTE or 5G NR [3], [4]. As its 20 km altitude is lower than that of communication satellites, a HAPS can directly connect smartphones to mobile communication services without needing special equipment such as satellite communication terminals.

In order to design HAPS cell configurations that efficiently support mobile communications, we need a radio wave propagation model that takes into consideration the terrain [5], the vegetation [6]–[11], urban areas, suburban areas [12], [13], building entry loss [14] and human body shielding [15], [16], etc., as shown in Fig. 2. [17] proposed a HAPS propagation loss model for urban and suburban ar-

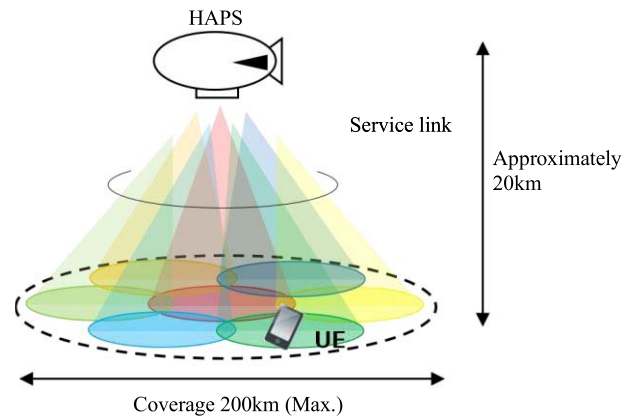


Fig. 1 High-altitude platform station (HAPS).

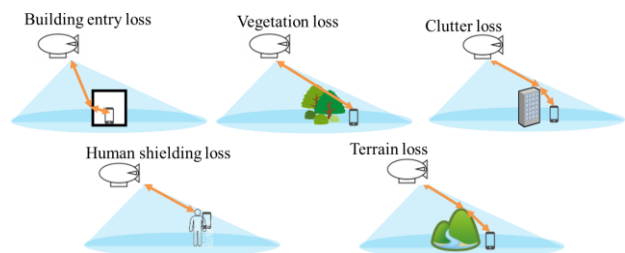


Fig. 2 HAPS propagation environment.

eas, and high elevation angle measurements were carried out using a helicopter to simulate assumed HAPS propagation environments. Regarding the HAPS system, some studies such as the system design of Gigabit, the cell configuration study, the cylindrical Massive MIMO system, and a cylindrical antenna design with beamforming method have been proposed and published in recent years [18]–[23].

Since rural areas have open swathes of land that have few homes or other buildings (i.e. there are few reflective objects around the mobile station (MS)), they are generally assumed to be multipath-sparse environments. Therefore, when the direct wave between a base station (BS) and MS is shielded by buildings, trees, human bodies, etc., the received power may be greatly degraded. Given this issue, it is necessary to clarify the characteristics of diffracted waves/waves scattered by isolated buildings, vegetation, and the human body.

New agenda item 1.4 for World Radiocommunication Conference (WRC) 23 was approved at WRC 19 for HAPS [24]. This agenda item requires consideration of the

Manuscript received July 16, 2021.

Manuscript revised November 26, 2021.

Manuscript publicized April 13, 2022.

<sup>†</sup>The authors are with SoftBank Corp., Tokyo, 135-00644 Japan.

a) E-mail: hideki.omote@g.softbank.co.jp  
DOI: 10.1587/transcom.2021EBP3109

use of high-altitude platform stations as IMT base station (HIBS) in the mobile service in certain frequency bands below 2.7 GHz, already identified for IMT, with global or regional studies of the bands 694–960 MHz, 1710–1885 MHz, and 2500–2690 MHz. The loss characteristics due to vegetation have been standardized as Recommendation ITU-R P.833-9 [6], however, the region and kinds of trees considered are limited. Also, there are few studies that address the seasonal characteristics of vegetation loss. The arrival angle characteristic in vegetated environments shows that the wave, coming from the direction of the transmitting antenna, is scattered as it passes through vegetation [8].

In this paper, we measure and analyze the vegetation loss of 1.47, 3.35, and 5.77 GHz at high elevation angles in different seasons in Japan. From the measured results, we clarify the relationship between transmission frequency and season in terms of vegetation loss and also propose a new vegetation loss model that can take account of the relationship between frequency and season. Moreover, in order to extend the lower limit of the frequency, we carry out field measurements using the 700 MHz band in the actual stratospheric environment in Kenya; the results predicted by the proposed model are compared to the measured results. The comparison shows that the proposed model is sufficiently valid in various areas including a stratospheric environment. To account for seasonal changes in vegetation and vegetation depth, we develop a statistical vegetation model from the proposed model.

## 2. Propagation Measurements

We measured excess loss due to vegetation and seasonal characteristics of vegetation loss in two vegetated areas in Japan and the total measurement points are 105. All measurements were carried out after stopping the measuring vehicle. Table 1 shows the field measurement parameters for the environment (1) and (2). Base on the measured results from the environment (1), we proposed a new vegetation loss model. An additional measurement in the environment (2) was carried out to confirm the validity of the proposed model that can be applied to other seasons. This section will introduce the measurement of the environment (1) and Sect. 3.3 will show the analyzed results of the environment (2).

According to the environment (1), the transmission signal is CW, the measurement frequencies are 1.47, 3.35, and 5.77 GHz, with transmission powers of 20, 10, and 10 W, respectively. The elevation angle is from 0.25 to 24.3 degrees and the vegetation depth is from 4.2 to 527.0 m, which can be calculated by recorded information of the height of the tree,  $h_v$ , horizontal vegetation depth,  $d_i$ , and the distance between the MS and tree,  $d_w$ , at each measurement point, the definition of each parameter is shown in Fig. 3.

In this measurement, as shown in Fig. 4(a), the BS antennas and measurement equipment were hung from an unmanned aerial vehicle. Figure 4(b) shows that the MS antenna was set on the measurement vehicle approximately

**Table 1** Field measurement parameters in Japan.

Environment (1)			
Frequency [GHz]	1.47	3.35	5.77
Transmitter Power [W]	20	10	10
BS/MS Antenna	Sleeve Antenna (Omni-Directional)		
Antenna Height [m]	MS:3, BS:80-800		
Transmitter Signal	CW		
Measured Season	Summer (July) Winter (Dec.)		
Horizontal Distance (from BS to MS) [m]	265 - 12601		
Elevation angle [deg.]	0.25 - 24.3		
Polarization	V - V		
Vegetation depth $d$ [m]	4.2 - 527.0		
Environment (2)			
Frequency [GHz]	3.35		
Transmitter Power [W]	10		
BS/MS Antenna	Sleeve Antenna (Omni-Directional)		
Antenna Height [m]	MS:3, BS:325-365		
Transmitter Signal	CW		
Measured Season	Spring (March)		
Horizontal Distance (from BS to MS) [m]	1600		
Elevation angle [deg.]	10.8 - 12.2		
Polarization	V - V		
Vegetation depth $d$ [m]	20 - 220		

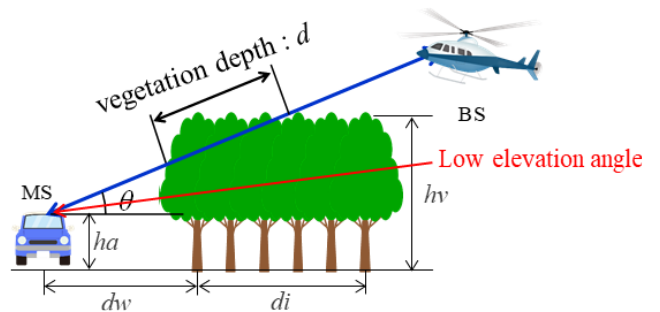
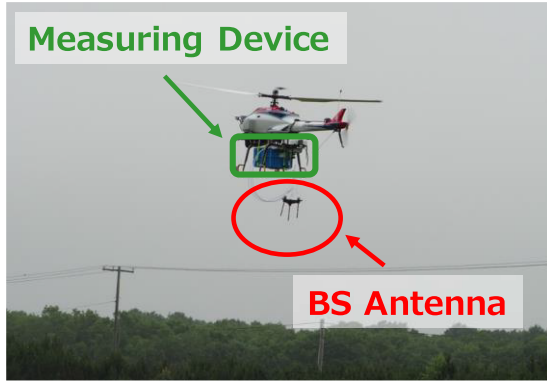
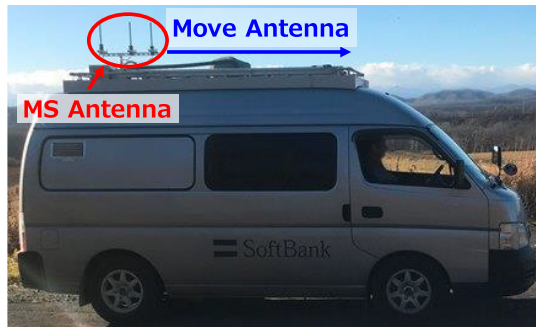


**Fig. 3** Vegetation loss environment.

3 m above the ground, and the BS antenna on the unmanned aerial vehicle varied in height from 80–800 m. All transmitting and receiving antennas were horizontal omnidirectional sleeve antennas. In order to consider the directivity of the used antennas to precisely calculate the vegetation loss in the analysis, the measurements were carried out in an elevation angle from 0.25 to 24.3 degrees within the 3 dB beamwidth of the antenna. For comparison, the measurements were also carried out at various LOS points within the same elevation range in the same area where the vegeta-



(a)



(b)

**Fig. 4** Measurement Configuration: (a) BS antennas and measurement equipment and (b) MS antennas on the roof of the measurement vehicle.

tion loss was measured. The results confirm that is consistent with the free-space basic transmission loss and thereby calculating the vegetation loss. Since the multipath fading due to multipath propagation may distort and attenuate the radio signal, it is required to eliminate the fading effect. In the measurement, we moved the MS antenna more than 20 wavelengths in the horizontal direction for each frequency by use of the traversing mechanism that is mounted on the top of the vehicle and averaged the received power. In addition, as shown in Fig. 5, the measurements were carried out in the same area in different seasons such as summer (July) when the leaves were plentiful and winter (December) when the leaves had already fallen.

### 3. Vegetation Loss Model

#### 3.1 Recommendation ITU-R P.833-9 Vegetation Loss Model

Figure 3 also shows a conceptual diagram of the vegetation loss model from Recommendation ITU-R P.833-9. The distance over which the direct path between the BS and MS passes through the vegetation depth is  $d$  [m], and the elevation angle is  $\theta$  [deg.]. The vegetation loss estimation equation standardized in Recommendation ITU-R P.833-9 is written as Eq. (1):

$$L(\text{dB}) = Af^B d^C (\theta + E)^G \quad (1)$$



(a)



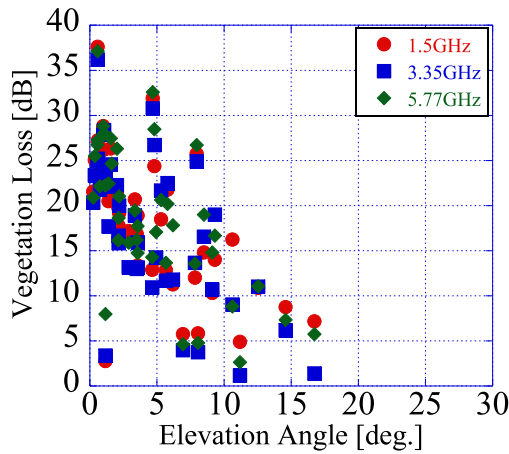
(b)

**Fig. 5** Tree leaf state with seasonal variation: (a) in summer and (b) in winter.

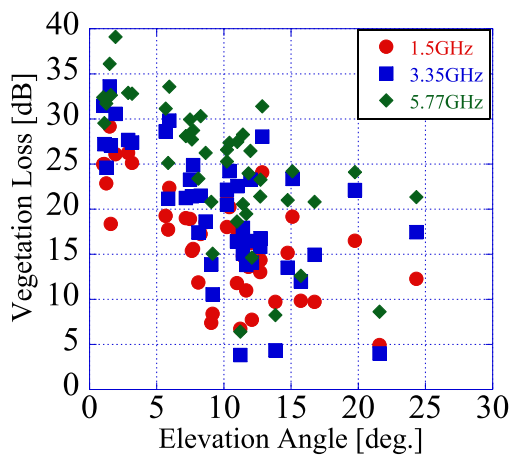
In the equation,  $f$  is the frequency [MHz],  $A, B, C, E,$  and  $G$  are constants for the region and kinds of tree, and all are dependent on frequency,  $f$ , and elevation angle,  $\theta$ . Note that Recommendation ITU-R. P.833-9 standardizes the values of  $A, B, C, E,$  and  $G$  for Austrian pine, as follows,  $A = 0.25, B = 0.39, C = 0.25, E = 0, G = 0.05$ .

#### 3.2 Measured Results

Figure 6 shows the measured results in the winter season and summer season for elevation angles from 0.25 to 24.3 degrees. From the results, we can find that the vegetation loss varies with elevation angle, season, and frequency. Figure 7 shows the measured values of vegetation loss at the same point in summer and winter plotted against elevation angle,  $\theta$ , defined using Recommendation ITU-R P.833-9, on the horizontal axis. All measurement conditions are the same except for the state of the leaves of the trees. Figures 7(a)–(c) show the measured results at the measurement frequencies of 1.47, 3.35, and 5.77 GHz. The following can be derived from Fig. 7: (1) The estimation results of the Austrian pine model standardized in Recommendation ITU-R P.833-9 are very different from the measured results of Japanese cedar. Thus, the model should be extended to cover different regions and kinds of trees. (2) Since the vegetation loss is greater in summer than in winter, vegetation loss has



(a)

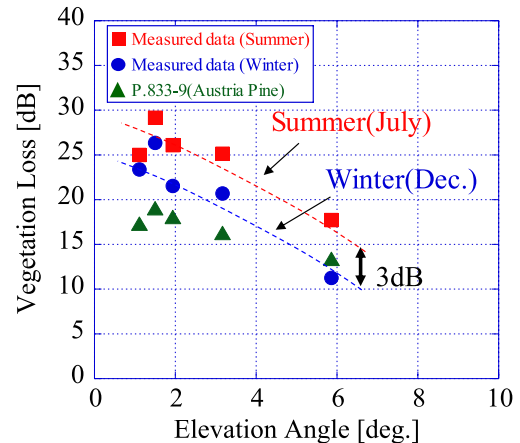


(b)

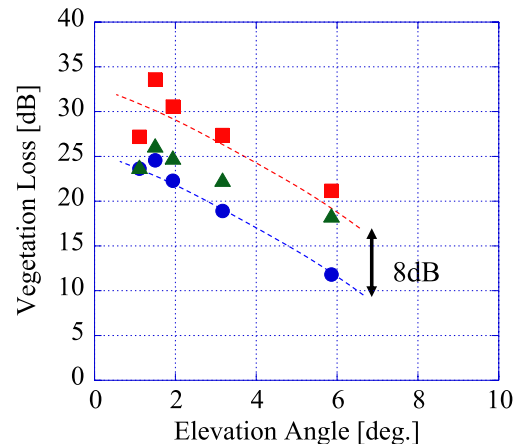
**Fig. 6** Measured vegetation loss: (a) in the winter season, (b) in the summer season.

seasonal variation reflecting leaf quantity. (3) The dashed line shows an approximate curve that represents the summer and winter measured results, respectively. It is found that the difference in vegetation loss between summer and winter is about 3 dB at 1.47 GHz, about 8 dB at 3.35 GHz, and about 11 dB at 5.77 GHz. Therefore, the seasonal variation of vegetation loss depends on frequency. In addition, the difference between summer vegetation loss and winter vegetation loss is greater at higher measurement frequencies; this is because the leaf cover has greater attenuation at higher frequencies.

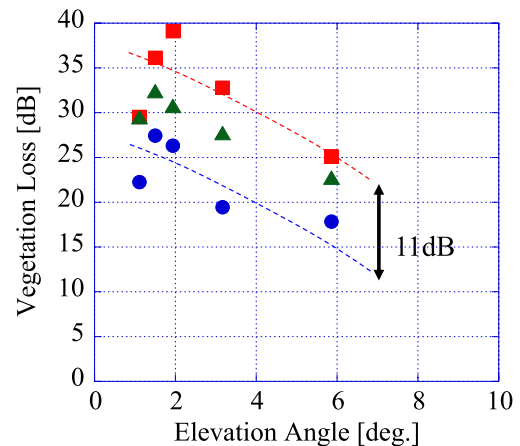
Figures 8(a) and (b) plot the estimation error obtained by subtracting the estimated value calculated according to Recommendation ITU-R P.833-9 from the measured vegetation loss at all measurement points in summer and winter, respectively. The elevation angle,  $\theta$ , in the measurements is from 0.25 to 24.3 degrees. From Fig. 8(a), the median estimation error in summer is about 5 dB regardless of frequency. These results confirm that the Austrian pine parameters standardized in Recommendation ITU-R P.833-9 cannot be applied to the vegetation loss created by Japanese trees. Figure 8(b) shows that the median estimated error



(a)



(b)



(c)

**Fig. 7** Measured vegetation loss: (a) 1.47 GHz, (b) 3.35 GHz and (c) 5.77 GHz.

values of vegetation loss in winter are 5 dB at 1.47 GHz, -3 dB at 3.35 GHz, and -5 dB at 5.77 GHz. A comparison of Figs. 8(a) and (b) confirms that there is seasonal variation in vegetation loss. Also, the estimation error in winter is large, this is because the estimation equation in Recommen-

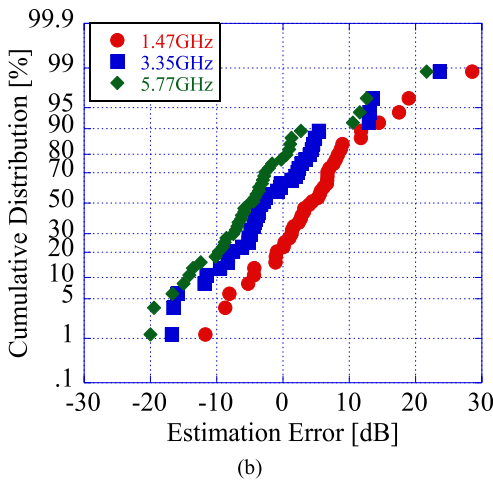
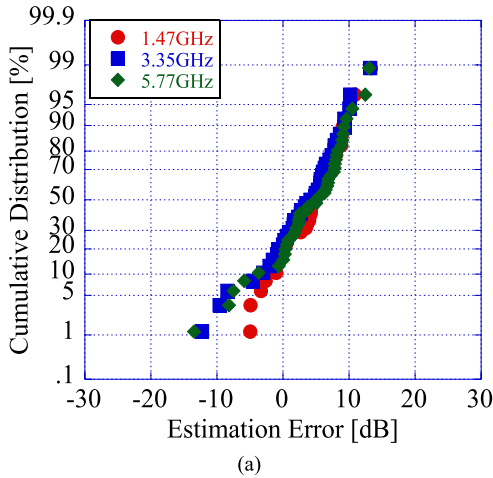


**Fig. 8** Estimation error given by Rec. ITU-R P.833-9 (Austrian Pine): (a) in the summer season and (b) in the winter season.

dition ITU-R P.833-9 does not take into account seasonal changes which is frequency dependent. Therefore, it is necessary to develop a new model that can correctly estimate seasonal and frequency characteristics.

### 3.3 New Vegetation Loss Model Considering Seasonal Variation

Figure 9 shows the comparison of the vegetation loss from 0 to 30 degrees in the winter season between measured results (red dots), the predicted results by Recommendation ITU-R P.833-9 (red line) and the proposed model (blue line), we can find some different points, for instance: when the elevation angle is less than 5 degrees, the predicted results are lower than measured results; when the elevation angle is more than 5 degrees, the predicted results are higher than measured results. Also, a particular issue is that no significant decrease in predicted results, when the elevation angle is more than 15 degrees. In fact, as the elevation angle increases, the  $d$  becomes smaller that also causes the vegetation loss to decrease, the image is shown in Fig. 3. However, according to the Recommendation ITU-R P.833-9, the veg-

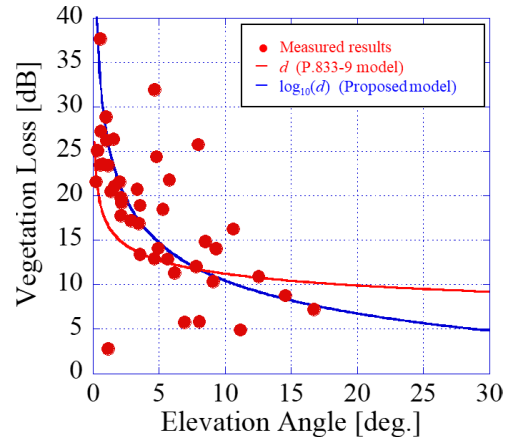


**Fig. 9** Comparison of the vegetation loss in the winter season.

etation loss does not decrease significantly with the increase of elevation angle. The blue line shows the predicted result by use of the proposed model when  $d$  is expressed by  $\log_{10}(d)$ , which is in a good agreement with the measured results. It is observed that the vegetation loss decreases when the elevation angle is more than 15 degrees, meaning the proposed model can accurately reproduce the phenomena as we mentioned above. By changing  $d$  to  $\log_{10}(d)$  and fine-tuning other parameters, the proposed model can fully reproduce the environment with high elevation angle. Based on these results, we propose a new model that establishes a relationship between frequency and season. The proposed estimation equation is given as Eq. (2):

$$L(\text{dB}) = Af^B \log_{10}(d)(\theta + E)^G - 4 \quad (2)$$

where:

- $f$ : frequency (MHz, 1400–6000 MHz);
- $d$ : vegetation depth (meters, 4.2–527.0 meters);
- $\theta$ : elevation (degrees, 0.25–24.3 degrees);
- $kh = |\text{Month} - 6.5|$ ;
- $\text{Month} = 1, 2, \dots, 12$ ;
- $A = 1.87$ ;
- $B = (0.302 - 0.0036kh)(f/1000)^{(0.0013 - 0.026kh)}$ ;
- $E = 0.01$ ;
- $G = -0.12$ .

Where the process of creating the proposed model is described in Appendix.

The key feature of the proposed model is that it can express the difference in seasonal variation (and its dependence on frequency) without greatly changing Recommendation ITU-R P.833-9. The number of leaves is assumed to maximize in mid-June (i.e.  $\text{Month} = 6.5$ ) in Japan. Since seasonal characteristics of vegetation loss depend on frequency,  $B$  is a function of  $f$ . It is possible to cover the southern hemisphere by swapping summer and winter in the seasonal term  $kh$ . Figure 10 shows the modeled estimation equation and the estimated error of the measured vegetation loss. Figure 10 confirms that the proposed model can well estimate the vegetation loss in the peak leaf summer season

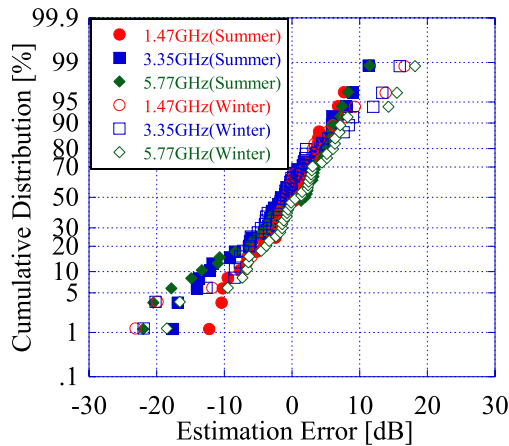


Fig. 10 Estimation error of the proposed model.

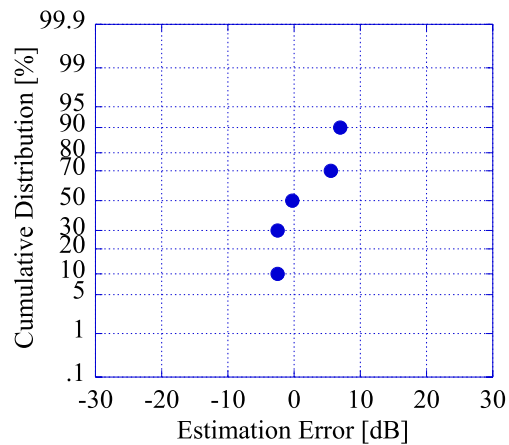


Fig. 11 Estimation error between the proposed model and measured results in the spring season.

and no leaf winter season such as in Japan.

In order to confirm the validity of the proposed model that can be applied to other seasons, an additional measurement in the environment (2) was carried out. The measurement parameter is shown in Table 1. The frequency is 3.35 GHz. The vegetation depth is from 20 to 220 meters and the elevation angle is from 10.8 to 12.2 degrees. To vary the vegetation depth and the elevation angle, the BS antenna is installed underneath the unmanned helicopter which is lifted from the top of the mountain and flies over the forest on the mountain slope. From Fig. 11, it is found that the proposed model can be applied to the spring season because the estimated error is 0 dB at the median value. Since we confirm the proposed model is applicable in the middle season that is between the peak leaf season and no leaf season, the proposed model can estimate the whole year. Figure 12 shows examples of estimated values of vegetation loss. Here,  $f = 2$  GHz, and *Month* is 1 or 12, 4 or 9, and 6 or 7.

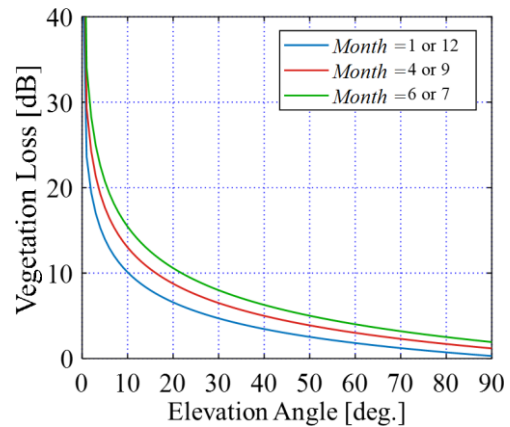


Fig. 12 Examples of estimated values of vegetation loss.

Table 2 Field measurement parameters in Kenya.

Frequency [GHz]	0.7
Antenna Height [m]	MS:2, BS:16400-18400
Transmitter Signal	LTE
Measured Season	Summer (Feb.)
Horizontal Distance (from BS to MS) [m]	1340-16900
Elevation angle [deg.]	39.8-84.0
Vegetation depth $d$ [m]	4.7 – 20.5

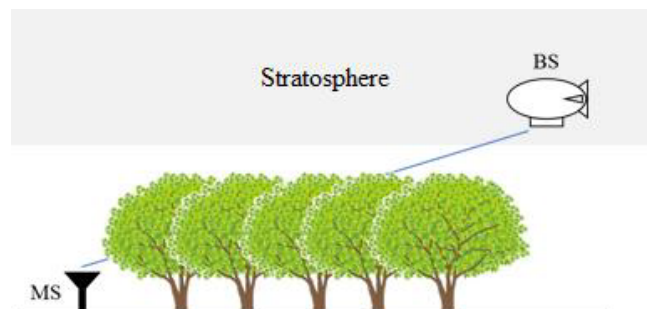


Fig. 13 Measurement in the stratosphere.

#### 4. Propagation Measurements in Stratospheric Environment

In order to further validate the proposed model, we carried out measurements in Kenya with the help of project Loon [25]. Kenya is a different environment from the area where the model was created. The total measurement points are 33. The field measurement parameters are shown in Table 2. Figure 13 the MS antenna was set approximately 2 meters above the ground, with the BS antenna on a balloon in the stratosphere. The received power was measured in the 700 MHz band while moving the MS antenna in the horizontal direction to eliminate the effect of fading. The received power was also measured at various elevation angles. As



Fig. 14 Example of the measurement environment.

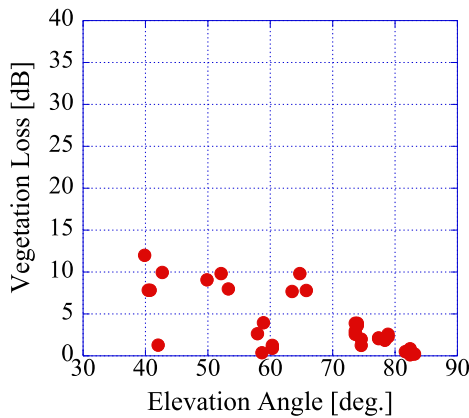


Fig. 15 Measured vegetation loss in Kenya.

Sect. 2 mentioned, to precisely calculate the vegetation loss in the analysis, it is required to consider the directivity of the used antennas. Since the elevation angle in the measurement is higher than the measurement which was carried out in Japan, we measured the received power in NLOS points and then compare with the results that were measured in LOS points where the environment and the elevation angle are the same as the NLOS point, and thereby calculating the vegetation loss, that means the effect of the directivity can be eliminated. Figure 14 shows an example of the measurement environment. Figure 15 shows the measured results for the elevation angles from 39.8 to 84.0 degrees. From the results, the vegetation loss decreases when the elevation angle approaches 90 degrees. Figure 16 shows the estimation error between the measured values and the estimated values calculated by Eq. (2) using the following values of empirical parameters  $A$ ,  $E$ , and  $G$ :

- $A$ : 1.5;
- $E$ : 0.01;
- $G$ : -0.12.

In order to avoid negative values, a value of  $-4$  is also used as a correction term in Eq. (3). Moreover, just changing parameter  $A$  of Japanese cedar from 1.87 to 1.5 for the proposed model can make estimation equation to well fit the measured results in Kenya. Here, the month is February.

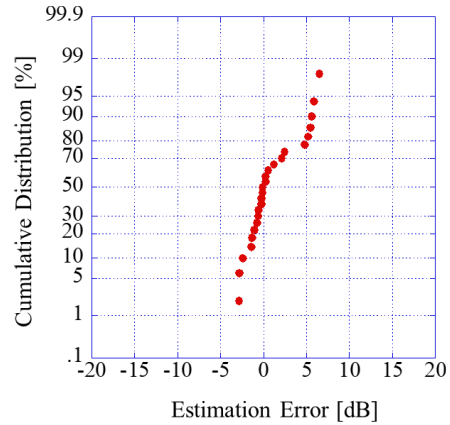


Fig. 16 The estimation error of predicted results for the proposed model in Kenya.

Table 3 Vegetation parameters.

Tree type	$A$	$E$	$G$
Japanese cedar	1.87	0.01	-0.12
Kenyan juniperus	1.5	0.01	-0.12

The measured areas in Kenya were in the southern hemisphere. For the value of  $kh$ , in the southern hemisphere,  $kh = 6 - |Month - 6.5|$  is used instead of  $|Month - 6.5|$ . Since the median value of the estimation error is 0 dB, which confirms that the proposed model is valid for the stratospheric environment, the applicable range of the high elevation angle to 84.0 degrees and extension of the lower limit of the frequency range to 700 MHz is proposed. Therefore, the proposed vegetation model for both Japan and Kenya is as follows:

$$L(\text{dB}) = Af^B \log_{10}(d)(\theta + E)^G - 4 \tag{3}$$

where:

- $f$ : frequency (MHz, 700–6000] MHz);
- $d$ : vegetation depth (meters, 4.2–527.0 meters);
- $\theta$ : elevation (degrees, 0.25–84.0 degrees);
- $kh = |Month - 6.5|$  (In the southern hemisphere,  $kh = 6 - |Month - 6.5|$  is used instead of left equation.);
- $Month = 1, 2, \dots, 12$ ;
- $B = (0.302 - 0.0036kh)(f/1000)^{(0.0013 - 0.0262kh)}$ ;
- $A, E, G$ : empirical parameters are shown in Table 3.

### 5. The Statistical Model

The proposed model described in Sect. 4 is a model in which the season and the vegetation depth are specified. On the other hand, if the proposed model is to be developed into a statistical model, it is necessary to take into account the seasonal changes and the vegetation depth that varies from the position. The proposed statistical model based on Eq. (4) is as follows:

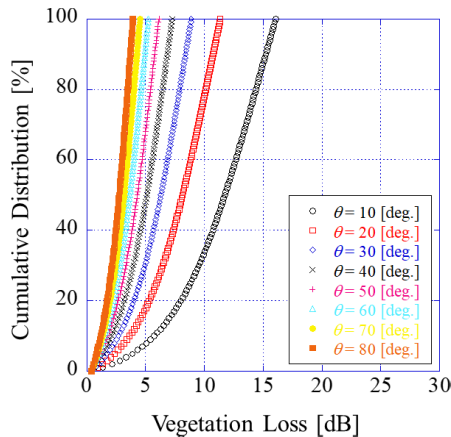


Fig. 17 Example of the vegetation loss calculated by the statistical model at varying elevation angles for 2 GHz.

$$L(\text{dB}) = Af^B \log_{10}(d)(\theta + E)^G - 4(p/100) + 0.4 \quad (4)$$

where:

$f$ : frequency (MHz, 700–6000 MHz);

$\theta$ : elevation (degrees, 1.0–84.0 degrees);

$d = 243(p/100)(\theta + 1)^{-0.93047} + 1$ ;

$kh = 5.5 - 5(p/100)$ ; [Note: The function is determined by the type of vegetation such as deciduous broadleaf forest.]

$B = (0.302 - 0.0036kh)(f/1000)^{(0.0013 - 0.0262kh)}$ ;

$A, E, G$ : empirical parameters.

$p$  is the probability including the time rate considering the season and the location rate considering the vegetation depth,  $d$ . For example, the vegetation loss is high when the season is in leafy seasons and  $d$  is large. On the other hand, the vegetation loss is low when the season is in not leafy seasons and  $d$  is small.  $A, E$  and  $G$  are determined for each area. For example, the values of Japanese cedar in Table 3 can be used for deciduous broadleaf forests such as those in Japan. Figure 17 shows an example of the vegetation loss calculated by the statistical model at varying elevation angles at 2 GHz.

## 6. Conclusion

In this paper, we measured the vegetation loss in summer and winter at 1.47, 3.35, 5.77 GHz, and in spring at 3.35 GHz in a Japanese rural area. It was confirmed that there was a seasonal variation in the vegetation loss due to the difference in the leaf state of Japanese deciduous trees and that the seasonal variation in vegetation loss was frequency dependent. Based on the measured vegetation loss characteristics, we developed a new vegetation loss model that considers seasonal variation and its dependence on frequency. We confirmed that the proposed model can estimate vegetation loss accurately for Japanese deciduous trees.

Further, we carried out field measurements in the stratospheric environment and compared the results predicted by the proposed model against the measured results.

The comparison showed that the proposed model is valid in various areas.

Additionally, we proposed a statistical vegetation model based on the proposed model. The proposed model is valid from 0.7 to 6 GHz, which covers almost the entire frequency band of WRC 23 A11.4.

## Acknowledgments

Part of this work is carried out under the grant, “R&D on efficient spectrum use technologies for wireless communications systems using HAPS (JPJ000254),” which is funded by the Ministry of Internal Affairs and Communications of Japan.

## References

- [1] S. Karapantazis and F. Pavlidou, “Broadband communications via high-altitude platforms: A survey,” *IEEE Commun. Surveys Tuts.*, vol.7, no.1, pp.2–31, May 2005.
- [2] R. Miura and M. Oodo, “Wireless communications system using stratospheric platforms: R and D program on telecom and broadcasting system using high altitude platform stations,” *J. Communication Research Laboratory*, vol.48, no.4, pp.33–48, Dec. 2001.
- [3] T. Fujii, “Expectation for the practical use of mobile communication system by using HAPS,” *IEICE Society Conf. 2018, BS-2-3*, Sept. 2018 (in Japanese).
- [4] A. Nagate, et al., “HAPS radio repeater system using the same system as terrestrial mobile communications system,” *IEICE Society-Conf. 2018, B-5-37*, Sept. 2018 (in Japanese).
- [5] Rec. ITU-R P.1812-4, “A path-specific propagation prediction method for point-to-area terrestrial services in the VHF and UHF bands,” 2015.
- [6] Rec. ITU-R P.833-9, “Attenuation in vegetation,” 2016.
- [7] S.L. Durden, J.D. Klein, and H.A. Zebker, “Radar measurement of L-band signal fluctuations caused by propagation through trees,” *IEEE Trans. Antennas Propag.*, vol.39, no.10, pp.1537–1539, Oct. 1991.
- [8] I.Z. Kovacs, P.C.F. Eggers, and K. Olesen, “Radio channel characterisation for forest environments in the VHF and UHF frequency bands,” *Proc. 50th IEEE VTC - Fall*, vol.3, pp.1387–1391, 1999.
- [9] J.C.R. Dal Bello, G.L. Siqueria, and H.L. Bertoni, “Theoretical analysis and measurement results of vegetation effects on path loss for mobile cellular communication system,” *IEEE Trans. Veh. Technol.*, vol.49, no.4, pp.1285–1293, July 2000.
- [10] M. Ghoraiishi, J. Takada, C. Phakasoum, T. Imai, and K. Kitao, “Azimuth and delay dispersion of mobile radio wave propagation through vegetation,” *EuCAP 2010*, 2010.
- [11] D. Ogata, A. Sato, S. Kimura, and H. Omote, “A study on vegetation loss model with seasonal characteristics,” *2020 14th European Conference on Antennas and Propagation (EuCAP)*, pp.1–4, 2020.
- [12] Rec. ITU-R P.1410-5, “Propagation data and prediction methods required for the design of terrestrial broadband radio access systems operating in a frequency range from 3 to 60 GHz,” 2012.
- [13] Rec. ITU-R P.2108-0, “Prediction of clutter loss,” 2017.
- [14] Rec. ITU-R P.2109-1, “Prediction of building Entry loss,” 2019.
- [15] A. Sato, D. Ogata, S. Kimura, H. Omote, and T. Hikage, “Measurement of human body blockage in HAPS communications with consideration of elevation angle,” *ISAP 2019*, 2019.
- [16] A. Sato, S. Kimura, H.Y. Lin, and H. Omote, “Propagation loss model of human body shielding in HAPS communications,” *ISAP2020*, Jan. 2021.
- [17] H. Omote, S. Kimura, H.Y. Lin, and A. Sato, “HAPS propagation loss model for urban and suburban environments,” *ISAP2020*, Jan.

2021.

[18] Y. Shibata, N. Kanazawa, M. Konishi, K. Hoshino, Y. Ohta, and A. Nagate, "System design of gigabit HAPS mobile communications," *IEEE Access*, vol.8, pp.157995–158007, Aug. 2020.

[19] Y. Shibata, N. Kanazawa, K. Hoshino, Y. Ohta, and A. Nagate, "A study on cell configuration for HAPS mobile communications," *IEEE VTC2019-Spring*, April 2019.

[20] K. Tashiro, K. Hoshino, and A. Nagate, "Cylindrical massive MIMO system with low-complexity angle-based user selection for high-altitude platform stations," *IEICE Trans. Commun.*, vol.E105-B, no.4, pp.449–460, April 2022.

[21] K. Tashiro, K. Hoshino, and A. Nagate, "Cylindrical massive MIMO system for HAPS: Capacity enhancement and coverage extension," *IEEE VTC2021-spring*, April 2021.

[22] S. Sudo, K. Hoshino, and Y. Ohta, "Basic evaluation of service link antenna for footprint fixation in HAPS system," *IEEE VTC2020-fall*, Oct. 2020.

[23] K. Hoshino, S. Sudo, and Y. Ohta, "A study on antenna beamforming method considering movement of solar plane in HAPS system," *IEEE VTC2019-Fall*, Sept. 2019.

[24] Res .247 (WRC 19), "Facilitating mobile connectivity in certain frequency bands below 2.7 GHz using high-altitude platform stations as international mobile telecommunications base stations," *The World Radiocommunication Conference (Sharm el-Sheikh, 2019)*, Egypt, 28 October to 22 November 2019.

[25] "TELKOM AND LOON ANNOUNCE PROGRESSIVE DEPLOYMENT OF LOON TECHNOLOGY TO CUSTOMERS FROM JULY," <https://telkom.co.ke/telkom-and-loon-announce-progressive-deployment-loon-technology-customers-july>

**Appendix: The Process of Creating the Proposed Model**

- 1) Before developing a new vegetation model, we check whether Rec. ITU-R P.833-9 can reproduce the measured results or not. Estimation error by Rec. ITU-R P.833-9 is about 2 dB at median value in the summer season as shown in Fig. 8(a).
- 2) After fine-tuning the parameter  $A$ ,  $B$ , and so on, the estimation error is to be 0 dB at the median value, which means the measured results in the summer season can be reproduced as shown in Fig. A-1.
- 3) However, if the value of the parameter is applied to the winter season, the estimation error at median value will be shifted as shown in Fig. 8(b).
- 4) From Fig. 8(b), we can know that the shift of the estimation error for each frequency is different. For instance, after fine-tuning parameter  $B$  which is a frequency coefficient, we can find that the estimation error (blue) at 5.77 GHz becomes 0 dB as the best case.
- 5) Figure A-3 shows the optimal  $B$  for each season and frequency. From the results, we can find that  $B$  is a function of  $f$  and  $kh$ , and also the function form is a power function.
- 6) Since, the function form of  $B$  was confirmed, the other parameters were adjusted.  $C$  was merged into  $A$ . For the reasons mentioned above,  $d$  was changed

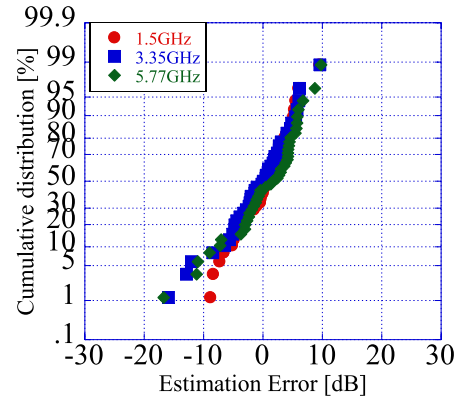


**Fig. A-1** Estimation error given by fine-tuning parameters  $A$  and  $B$  in the summer season.

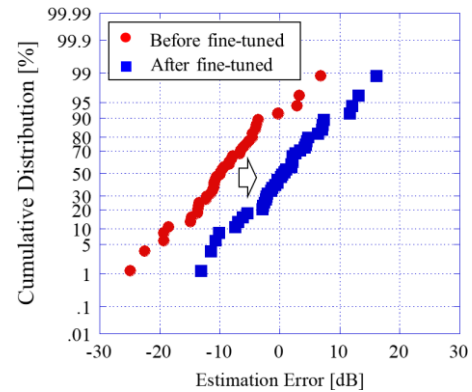


**Fig. A-2** Estimation error given by fine-tuning  $B$  in the winter season.

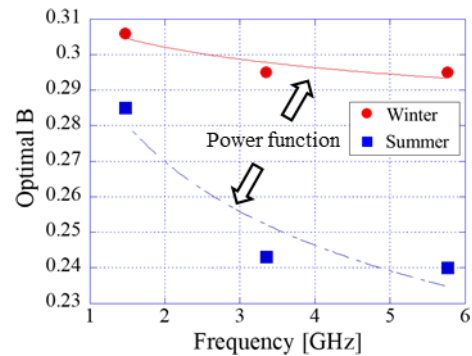


**Fig. A-3** Optimal  $B$  for summer and winter seasons.

to  $\log_{10}(d)$ , and the proposed model was developed by use of the correction term  $-4$  and other parameters that were fine-tuned. Here, this model is assumed to apply to target frequencies from 0.7 to 5.7 GHz and target elevation angle from 0–90 degrees. It is also assumed that the vegetation loss decreases to close to zero when the elevation angle is large. To ensure this and avoid negative values, a value of  $-4$  is used as a correction term. When the correction term is constant, the results for 1.5–5.7 GHz show a good agreement with the predicted results. This result also agrees well with the re-

sults at 0.7 GHz. From the above results, we set  $-4$  as a constant.



**Hideki Omote** was born in Iwatsuki City, Saitama Prefecture, in 1973. He received his B.S. and M.S. degrees from the University of Nagoya, Japan, in 1997 and 1999, respectively. He joined Japan Telecom Co, LTD. (currently, Softbank Corp.) in 1999. Since then, he has been engaged in the research of radio propagation for mobile communication systems. He also has been engaged in the standardization of radio propagation for mobile communication in ITU-R SG3. He is currently directing the New Technology R&D Department of Technology Research Laboratory at Softbank Corp.

In 2017, he also joined the Tokyo Institute of Technology, where he researches radio propagation and modeling. Mr. Omote is a member of IEICE.



**Akihiro Sato** was born in Yamagata, Japan, in 1985. He received the B.S. degree from the University of Yamagata. He joined Technology Research Laboratory at Softbank Corp. in 2018. Since then, he has been engaged in the research of radio propagation for mobile communication systems. He also has been engaged in the standardization of radio propagation for mobile communication in ITU-R SG3. Mr. Sato is a member of the Institute of Electronics, Information, and Communication Engineers (IEICE).



**Sho Kimura** was born in Wakayama, Japan, in 1991. He received the B.S. degree from Keio University. He joined Technology Research Laboratory at Softbank Corp. in 2014. Since then, he has been engaged in the research of radio propagation for mobile communication systems. Mr. Kimura is a member of the Institute of Electronics, Information, and Communication Engineers (IEICE).



**Shoma Tanaka** was born in Chiba, Japan, in 1995. He received the B.E. degree in Electrical and Electronic Engineering from the Tokyo Metropolitan University in 2018, and the M.E. degree in Electrical and Electronic Engineering from the Tokyo Institute of Technology in 2020. He joined Technology Research Laboratory at Softbank Corp. in 2020. Since then, he has been engaged in the research of radio propagation for mobile communication systems. He also has been engaged in the standardization of

radio propagation for mobile communication in ITU-R SG3. Mr. Tanaka is a member of the Institute of Electronics, Information, and Communication Engineers (IEICE).



**HoYu Lin** was born in Taipei, Taiwan, in 1983. He received the B.S. and M.E. degree in electronic engineering from Southern Taiwan University, Tainan, Taiwan, in 2007 and 2009, respectively, and the D.E. degree from Chiba University, Chiba, Japan, in 2014. His research interests include electrically antennas for mobile communications, BAN, and also radio propagation. He joined Technology Research Laboratory at Softbank Corp., in 2019. Since then, he has been engaged in the research of radio propa-

gation for mobile communication systems. He also has been engaged in the standardization of radio propagation for mobile communication in ITU-R SG3. Dr. Lin is a member of the Institute of Electronics, Information, and Communication Engineers (IEICE), Japan, and IEEE Antennas and Propagation Society (IEEE AP-S). He was the recipient of the 2014 IEEE Antennas and Propagation Society (IEEE AP-S) Tokyo Chapter Young Engineer Award.